

Investigation of the Optical Properties in the Infrared Region of PbS Thin Films

Bao Quy Le

School of Mechanical Engineering, Hanoi University of Science and Technology,
1 Dai Co Viet, 100000 Hanoi, Vietnam

Dat Tran Quang, Vi Le Dinh

Le Quy Đon Technical University, Hanoi 100000, Viet Nam
dattq@lqdtu.edu.vn; vild@lqdtu.edu.vn

Phuc Duong Van, Huan Vuong Van

School of Mechanical Engineering, Hanoi University of Science and Technology,
1 Dai Co Viet, 100000 Hanoi, Vietnam
phuc.dv205789@sis.hust.edu.vn; huan.vv205667@sis.hust.edu.vn

Hoat Phung Dinh, Tuan Nguyen Van, Thin Pham Van

Le Quy Đon Technical University, Hanoi 100000, Viet Nam
Tuannv@lqdtu.edu.vn; thinpv@lqdtu.edu.vn

Cuc Nguyen Thi Kim

Precision Engineering & Smart measurements Lab, School of Mechanical
Engineering, Hanoi University of Science and Technology,
1 Dai Co Viet, 100000 Hanoi, Vietnam
cuc.nguyethikim@hust.edu.vn

Abstract: Thin film's optical performance is governed by factors. These include optical and luminescent properties, and material structure. However, there are currently few domestic studies investigating these properties, especially the optical properties of thin films in the infrared region. PbS is a promising material for infrared sensing applications due to its high bandgap energy, which corresponds to the infrared spectrum. The goal of this research is to

explore the optical properties of PbS thin films and understand their potential applications in infrared sensors and imaging cameras. Investigate the properties of this film through simulation and compare them with experimental results. The results demonstrate the adjustable optical properties of PbS thin films in the infrared region, highlighting the effective absorption and emission of infrared light. The absorption spectrum indicates that PbS is a suitable candidate for infrared camera sensors. The structure in the study consists of three layers: Au / PbS / MZO. The photoelectric performance of PbS film, as already investigated, achieves high conversion values in the infrared region with parameters of doping film 10^{17} cm^{-3} , thickness $0.2 \mu\text{m}$, and bulk defect density 10^{16} cm^{-3} , temperature $300 \text{ }^\circ\text{K}$. With these optimal values, when imitating, a PCE photovoltaic conversion value of up to 24% is obtained. These findings minimize the possibility of errors during the experiments and show the potential for using PbS as a promising material for various infrared applications, including infrared sensors and solar cells. Further research may focus on optimizing manufacturing processes and exploring the performance of PbS-based infrared sensors. All reported studies were conducted using the SCAPS-1D simulation platform.

Keywords: PbS; thin films; luminescence; optical properties; infrared sensors

1 Introduction

With a direct bandgap of 0.4 eV, lead sulfide (PbS) is one of the most significant IV-VI narrow bandgap compounds that is frequently used in infrared sensors. According to a study [1], the stimulated Bohr exciton radius of PbS can achieve 18 nm. PbS's infrared optical characteristics suggest that it could find use in infrared sensors, imaging, and both military and civilian applications. PbS has been studied and used in solar cells for a long time. A power conversion efficiency (PCE) of more than 13% has been obtained by PbS colloidal quantum dot (CQD) thin films based on MgZnO (MZO) and TiO₂ electron transport layer (ETL) absorbing tetrabutylammonium iodide (PbS-TBAI) [2]. According to a different study, lead sulfide quantum dots (QDs) are becoming increasingly considered promising candidates for the next generation of flexible and affordable light-absorbing materials that are appropriate for waveguide-based optical separation because of their wide adjustable bandgap, high absorption coefficient, relatively simple solution processing, and stability in air [3]. Because of their unique structure and size-dependent properties, nanostructured PbS crystals (NC) show exceptional flexibility and offer promise for applications in upcoming nano-electronic and nano-optoelectronic devices as well as conventional optical devices [4]. The optical qualities of PbS thin films can be customized for particular uses by adjusting the film thickness. Another study on a hybrid phototransistor structure shows benefits concerning rapid electron transport through the MoS₂ layer, effective charge separation at the p-n interface, and tunable light absorption across the entire optical/IR spectrum. The hybrid phototransistor structure is constructed from up of

PbS quantum dot (QD) adhesive particles and multiple layers of MoS₂. Based on back gate-dependent sensitivity, experimental results demonstrate a feedback capability of up to 10⁶ AW⁻¹ [5].

In a different study conducted in 2016, C. Hu et al. employed 2D WSe₂ and bright-sensitive PbS QDs to create hybrid QD/2D-WSe₂ semiconductor balls for broad bandwidth and high-performance optical waveguide separation. Up to two times the AW-1 feedback capacity was demonstrated by this device [6]. The effects of replacing MoS₂/Wse₂ with MZO on the fluctuation in PbS film characteristics in the infrared range were examined. Zang et al. investigated the MZO layer from a solar cell pin structure [2]. A recent article investigated and designed thin films in infrared sensors with layers including Au, MoS₂ and FTO. This article systematically simulates different physical properties of the MoS₂ absorption layer. The components changed include thickness, doping, bulk defect density and obtained optimized values of 1 μm, 10¹⁸ cm⁻³, 10¹⁵ cm⁻³. These simulations were performed under 700 nm wavelength spectrum illumination, boasting a responsivity of 0.37 AW⁻¹ and a detectivity of 3.27x10¹⁴ Jones [7]. In this research, the properties of the PbS layer were simulated and investigated in terms of thickness, doping density, wavelength and temperature. Temperature and bandgap are also two crucial factors that affect the optical properties of PbS thin films. So, by analyzing the variations in the optical properties of PbS films with parameters including film thickness, simulation method, and substrate layers, we may have a better knowledge of the factors influencing the optical characteristics of PbS thin films.

In summary, this study aims to provide a comprehensive exploration of the optical properties of PbS thin films in the infrared spectrum. Three layers are included in this study: Au/PbS and MZO. By comprehending their luminous properties and investigating the factors influencing their performance, we can harness the potential of PbS thin films for various infrared applications. This paper will consist of the following sections: 1) Introduction, 2) Method, 3) Result and discussion, 4) Conclusion.

2 Method

Here, the properties of PbS thin film materials using the SCAPS-1D Simulation software were simulated. The device is configured as a three-layer structure, presenting a transition metal dichalcogenides TMDC-QD hybrid semiconductor consisting of adhesive p-type PbS quantum dots and several layers of n-type MZO. The device consists of three layers Au/PbS/MZO. Au is an electrode in the structure. PbS is a type p semiconductor. MZO is the electron transport layer (ETL).

This combination benefits from bright light absorption and modified quantum dot sizes, high waveguide flexibility in the MZO layer, and detector operation in the

depletion mode of the channel, allowing for minimal leakage current. The structure of the PbS thin film is depicted in Figure 1 a. Incident light is absorbed in the PbS QD layer, and the photo-excited electron-hole pairs are separated at the p-n junction interface between MZO and PbS. While the hole carriers remain within the QD layer, the electrons move through the MZO channel controlled by the applied bias voltage. The key feature of this hybrid structure is that the current can be controlled by an appropriate gate voltage. By increasing the voltage (V), the MZO channel enters the accumulation region. For real light detection applications, the operation mode of interest is in the depletion region, providing minimal electrical conductivity. While the hole carriers are retained within the PbS volume, the electrons are transferred multiple times through the MZO channel. The applied gate voltage will control the current level under both illuminated and dark conditions to enhance the sensitivity of the hybrid. The wavelength range surveyed is from 700 nm to 1000 nm, with the simulation using the AM 1.5 G model. The MZO layer parameters are cited from the work of Zang *et al.*, 2017 [8].

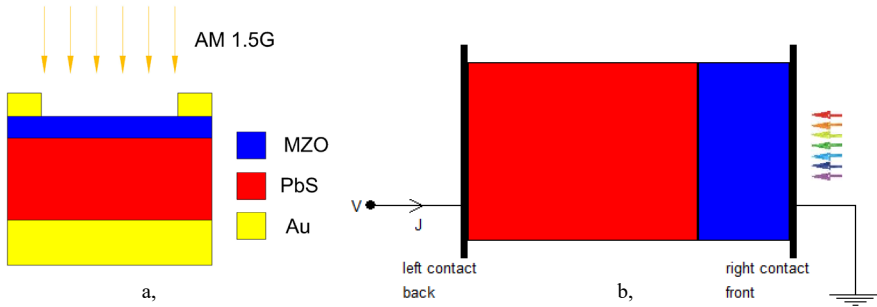


Figure 1

Structure of the thin film (a.)

Model figure from SCAPS simulation. Red: PbS; blue: MZO (b.)

The absorption coefficient of PbS used in the simulation is taken from the reference [2] and is illustrated in Figure 2. The material layer parameters in Table 1 are extracted from the work of [5]. The output results are in numerical form and plotted on graphs.

The absorption factor is an important parameter for simulation. The absorption coefficient of MZO was considered, calculated using the equation taken from:

$$\alpha(h\nu) = \left(\alpha_0 + \beta_0 \frac{E_g}{h\nu} \right) \sqrt{\frac{h\nu}{E_g} - 1} \quad (1)$$

Where, $\alpha(h\nu)$ is the absorption coefficient, E_g is the bandgap, and $h\nu$ is the photon energy. Here, $\alpha_0 = 10^5 \text{ cm}^{-1}$ and $\beta_0 = 10^{-12} \text{ cm}^{-1}$ is used during simulations. This model assumes that $\alpha(h\nu) = 0$ for $h\nu < E_g$

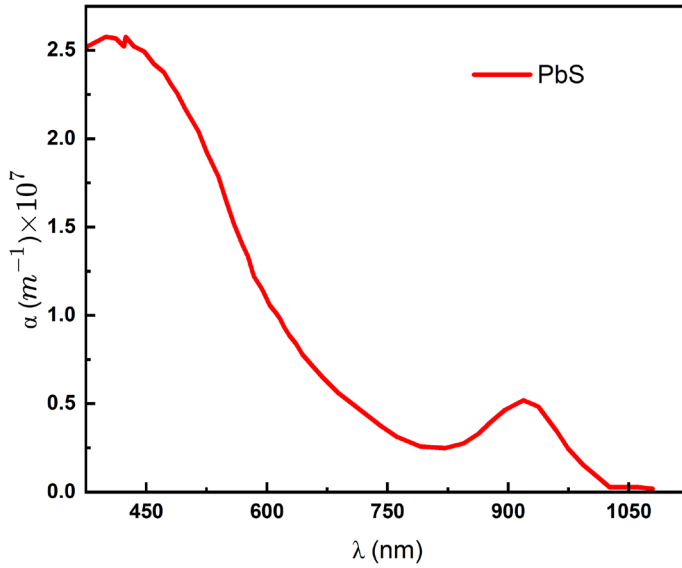


Figure 2

The wavelength- dependent absorption coefficient of PbS was used in the simulations [2]

Table 1
Properties of front and back contact

Parameters	Front contact	Back contact
Surface recombination velocity of electron S_n	1×10^7	1×10^4
Surface recombination velocity of hole S_p	1×10^4	1×10^7
Transmission coefficient T(%)	1	0
Reflection coefficient R(%)	0	1

Table 2
Details of SCAPS simulation used parameters

Parameters	PbS	MZO
Thickness (μm)	0.1 - 1.0	0.08
Bandgap (eV)	1.4	3.35
Electron affinity (eV)	4.35	4.0
Dielectric Permittivity (relative)	10	66
CB effective density of states (cm^{-3})	1×10^{18}	1×10^{19}
VB effective density of states (cm^{-3})	1×10^{18}	1×10^{19}
Electron mobility ($cm^2 V^{-1} s^{-1}$)	5×10^1	5×10^{-2}
Hole mobility ($cm^2 V^{-1} s^{-1}$)	1×10^1	5×10^{-2}
ND grading (uniform) shallow uniform donor density ND (cm^{-3})	0	1×10^{17}

NA grading (uniform) shallow uniform acceptor density NA (cm^{-3})	1×10^{17}	0
Absorption coefficient	Figure 2	SCAPS model

3 Result and Discussion

The simulation results from the electronic-photonic model indicate that the Conduction Band Minimum (CBM) of the Electron Transport Layer (ETL) significantly influences the photovoltaic performance of the device (Figure 3). An ETL with a higher CBM can provide better energy level alignment, maximizing the electron transfer process between the Quantum Dots (QD) and ETL. However, if the CBM has excessively high energy, the electron separation process may be affected [4]. The smoother band alignment at the ETL/QD interface is observed in the solar cell based on MZO-NC, potentially aiding the electron extraction process from QD to MZO-NC, reducing interfacial charge recombination. Short-circuit current density (J_{sc}) and open-circuit voltage (V_{oc}) are also investigated.

Figures 3, 4 and 5 show the dependence of V_{oc} and FF on the thickness of the thin film. The FF is a measure of the squareness of the I-V curve of PV equipment, which is mainly affected by the serial resistance of the cell [2]. The overall serial resistance of the device includes the resistance of individual semiconductor layers, their related interfaces, and metal-semiconductor contacts.

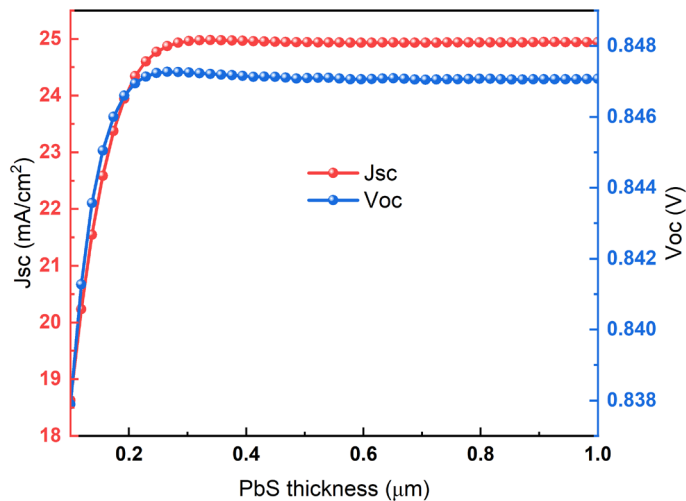


Figure 3
J-V characteristics

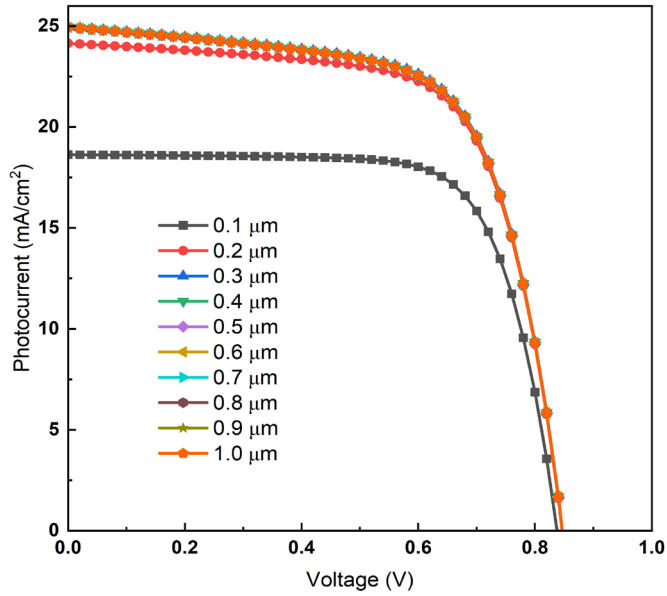


Figure 4
 V_{OC} and J_{SC} variation for various PbS layer thickness

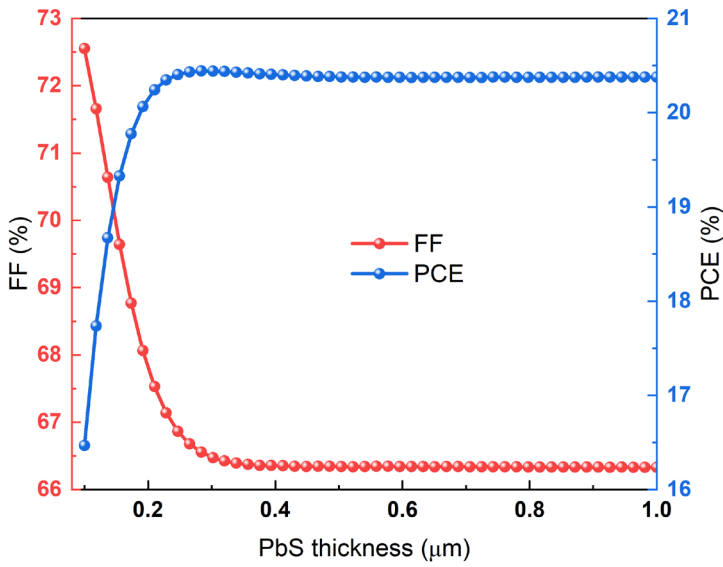


Figure 5
 FF and PCE for different thicknesses of PbS

After the simulation obtained, the FF coefficient tended to decrease, while the V_{oc} tended to increase in the range of $0.1 \div 1 \mu\text{m}$. From the above figures, the selected PbS thin film thickness parameter for simulation is $0.2 \mu\text{m}$ because with this value it is easy to apply fabrication methods such as spray coating.

In this investigation, PbS is a type p semiconductor, doping is also one of the principal factors affecting the performance of infrared sensors. With the initial parameters, we simulated the change in doping acceptance concentration between 1×10^{14} and $5 \times 10^{17} \text{ cm}^{-3}$ achieving the results as shown in Figure 6 and 7. Figure 7 shows that V_{oc} tend to increase as the concentration of doping receptors increases while J_{sc} decreases. V_{oc} tends to increase slightly between 1×10^{17} to $5 \times 10^{17} \text{ cm}^{-3}$, considering the difficult in device fabricating so the doping density of $1 \times 10^{17} \text{ cm}^{-3}$ is chosen to be optimizing for futher simulation.

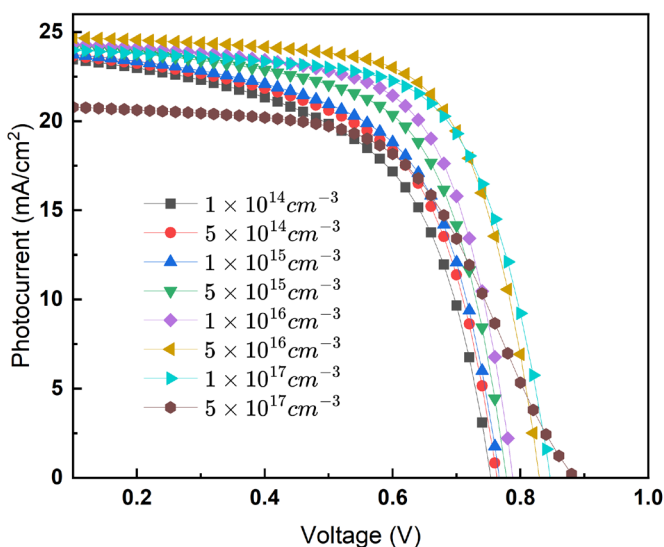


Figure 6

J-V characteristics device performance for various doping concentration of PbS layer

With the simulation parameters optimized above, the PbS layer on the efficiency of the device was simulated and investigated the impact of the defect density. Values vary in the range $1 \times 10^{13} \div 1 \times 10^{17} \text{ cm}^{-3}$, and device performance is shown in Figures 8 and 9. Performance begins to deteriorate with increasing defect density of the PbS layer, which is due to the carrier recombination generated and not due to an increase in defect density, which significantly reduces the efficiency of the device. Therefore, the defect density on the PbS layer also plays an important role in the detector's performance. From Figure 8, with values $1 \times 10^{13} \text{ cm}^{-3}$ and $1 \times 10^{14} \text{ cm}^{-3}$ the device performance is almost the same. However, with optimal values and the view of ease of fabrication, the bulk defect density of $1 \times 10^{16} \text{ cm}^{-3}$ was used to simulate the photodetector.

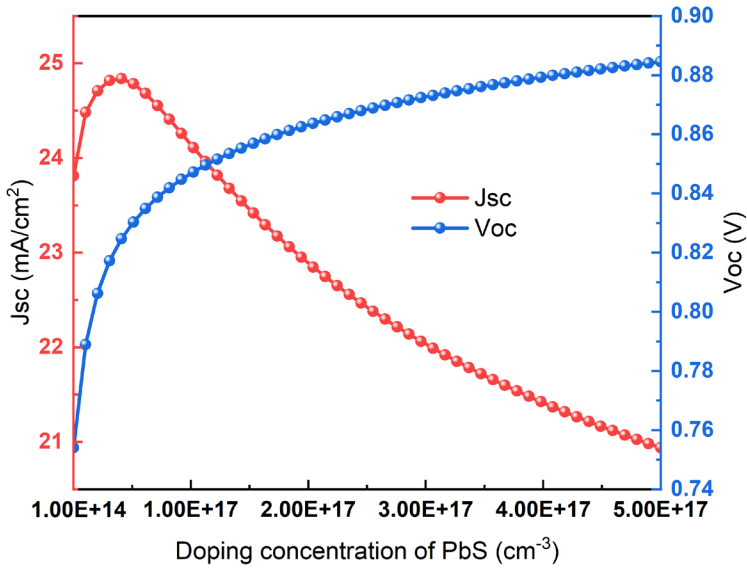


Figure 7

V_{oc} and J_{sc} when PbS class doping concentration changes

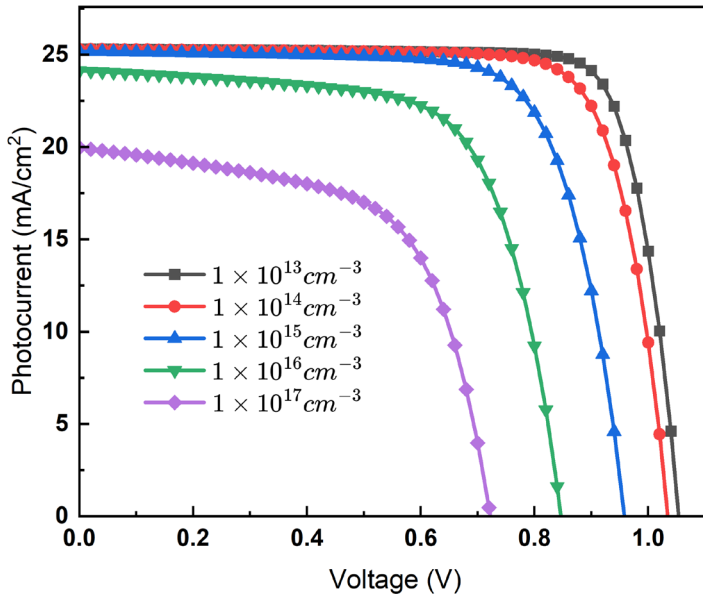


Figure 8

Effect of bulk defect on device performance via J-V characteristics

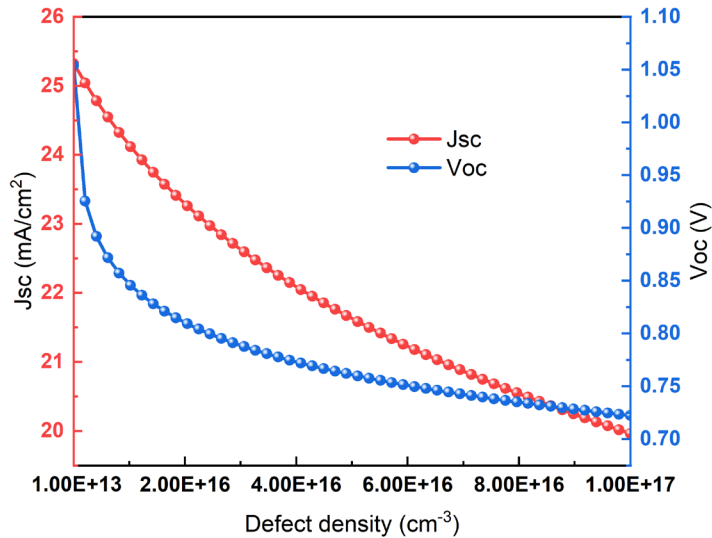


Figure 9

V_{oc} and J_{sc} due to the effect of bulk defect on device performance

Simulation parameters are obtained with an optimum film thickness of 0.2 μm , an acceptable doping density of $1 \times 10^{17} \text{ cm}^{-3}$ and a bulk defect density of $1 \times 10^{16} \text{ cm}^{-3}$. Consider cases where the structure is illuminated and in dark conditions. The darkness and optical current of the optimized device are shown in Figure 10, and the photo-to-dark current ratio is about $1 \times 10^{-10} \text{ mA/cm}^2$. The energy band alignment of the device is shown in Figure 11. From the ETL absorption layer, the energy band E_c tends to decrease due to the disorderly movement of electrons at bulk defect density of $1 \times 10^{16} \text{ cm}^{-3}$. This reduction in energy level is as a result of limited conduction of light-generated electrons in the absorbing layer.

After obtaining optimal results in thickness and doping, we simulated the influence of the light source on the performance of the PbS layer. With the initial parameter surveyed, the 1.5 G AM source has a wavelength range of 700 nm \div 1000 nm. The result is obtained as shown in Figure 12. With AM 1.5 G there is a much lower J_{SC} than the rest of the wavelengths. However, at 900 nm illumination, PCE was obtained up to 24%.

The photodetector has reached a maximum photocurrent of 42 mA/cm² under the illumination of AM 1.5 G. The effect of temperature on the optical current and V_{oc} of Figure 13.

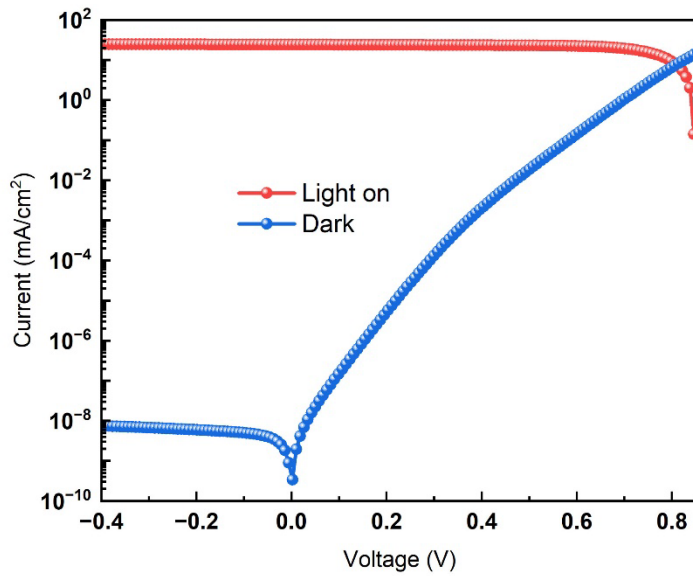


Figure 10

J-V curves of the simulated photodetector with and without light illumination

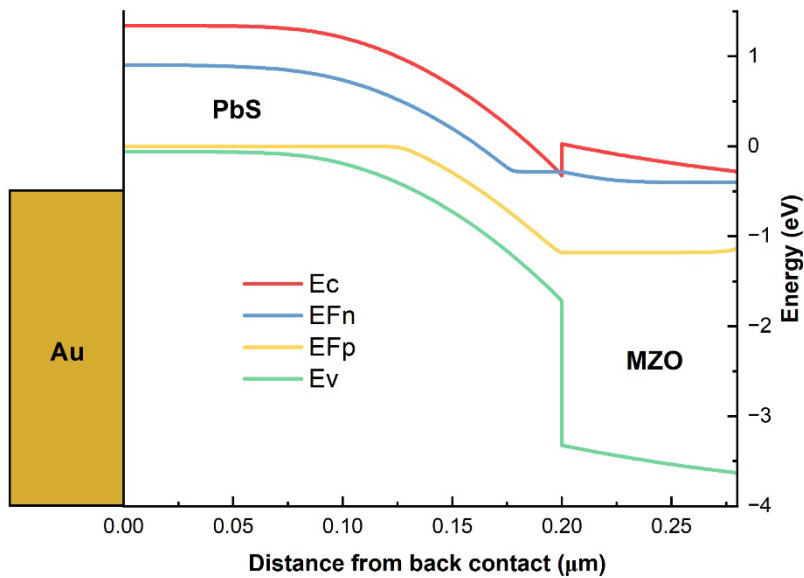


Figure 11

Band diagram of the optimized device with and without illumination of light

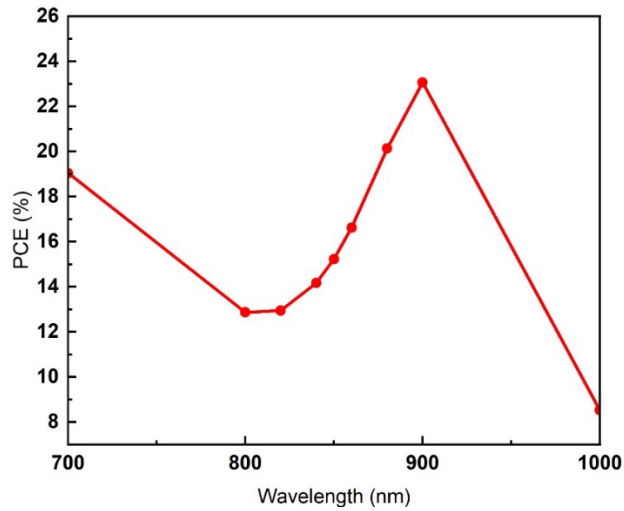


Figure 12

PCE with illumination sources of different wavelengths

After the survey, we found that the photovoltaic conversion efficiency (PCE) varies depending on the temperature as shown in Figure 14. In the temperature survey range from 280°K to 480°K, the photovoltaic conversion efficiency increases rapidly and achieves high efficiencies in a temperature of 300°K. After this interval, this performance tends to decrease.

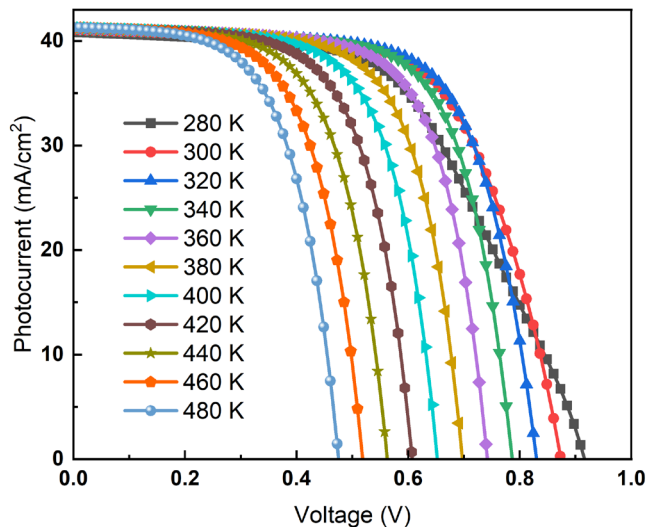


Figure 13

The conversion efficiency dependant on temperature

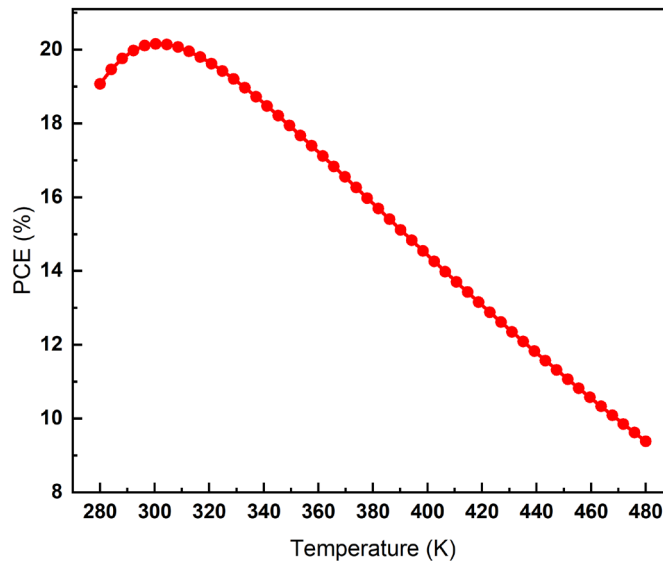


Figure 14

Photovoltaic conversion efficiency depends on temperature

Conclusions

In this study, the photodetection properties of PbS thin films were investigated in the infrared region. The PbS membrane was assessed with a single layer and an additional layer of MZO, achieving useful results for the experiment. The results indicate that thin PbS films exhibit strong luminescent properties in the infrared region. After simulation, the optimal parameters of PbS were obtained such as film thickness $0.2 \mu\text{m}$, doping density 10^{17}cm^{-3} , bulk defect density 10^{16}cm^{-3} , projection source with wavelength 900nm and optimum temperature about 300°K . When stimulated by infrared light, the luminescent intensity of the membrane increases significantly, suggesting potential applications in infrared sensors and solar cells. The photovoltaic conversion efficiency of the device is achieved up to 24%. In summary, the study of the photodetection properties of PbS thin films in the infrared region has provided essential information about luminescence properties, sensitivity, and optimization requirements for PbS thin films. These results will contribute to the correct experiment, minimizing errors during testing. From simulation to testing to developing PbS-based devices for infrared applications and exploring their potential in areas related to sensors and optoelectronics. Further research is needed to maximize the luminescence characteristics and performance of thin PbS films in the infrared region.

Acknowledgement

This research is funded by Hanoi University of Science and Technology (HUST) under project number T2023-PC-012.

References

- [1] K. S. S. Rajathia, K. Kirubavathib, “Preparation of nanocrystalline Cd doped PbS thin films and their structural and optical properties,” *J. Taibah Univ. Sci.*, pp. 1296-1305, 2017
- [2] J. M. Rahul Pandeya, Arrik Khannab, Karanveer Singhb, Sumit Kumar Patelb, Hardeep Singhb, “Device simulations: Toward the design of > 13% efficient PbS colloidal quantum dot solar cell Rahul,” *Sol. Energy*, Vol. 207, pp. 893-902, 2020
- [3] J. W. Zhenwei Ren, Jiankun Sun, Hui Li, Peng Mao, Yuanzhi Wei, Xinhua Zhong,* Jinsong Hu,* Shiyong Yang, “Bilayer PbS Quantum Dots for High-Performance Photodetectors,” *Adv. Mater.*, Vol. 29, No. 33, 2017
- [4] N. O. B. Zamin Mamiyev, “PbS nanostructures: A review of recent advances,” *Mater. Today Sustain.*, Vol. 21, No. 100305, 2023
- [5] G. K. Dominik Kufer, Ivan Nikitskiy, Tania Lasanta, Gabriele Navickaite, Frank H. L. Koppens, “Hybrid 2D–0D MoS₂–PbS Quantum Dot Photodetectors,” *Adv. Mater.*, Vol. 27, No. 1, pp. 176-180, 2014
- [6] H. S. Chao Hu, Dongdong Dong, Xiaokun Yang, Keke Qiao, Dun Yang, Hui Deng, Shengjie Yuan, Jahangeer Khan, Yang Lan and J. Tang, “Synergistic Effect of Hybrid PbS Quantum Dots/2D-WSe₂ Toward High Performance and Broadband Phototransistors,” *Adv. Mater.*, Vol. 27, No. 2, 2016
- [7] N. Roy, “Design and performance evaluation of MoS₂ photodetector in vertical MSM configuration,” *Opt Mater (Amst)*, Vol. 148, Feb. 2024, doi: 10.1016/j.optmat.2023.114817
- [8] E. M. J. J. Xiaoliang Zhang, † Pralay Kanti Santra, Lei Tian, † Malin B. Johansson, † Håkan Rensmo, “Highly Efficient Flexible Quantum Dot Solar Cells with Improved Electron Extraction Using MgZnO Nanocrystals,” *Am. Chem. Soc.*, pp. 8478-8487, 2017